URC97111

THE USE OF DECENTRALIZED CONTROL IN THE DESIGN OF A LARGE SEGMENTED SPACE REFLECTOR

by

Helen Ryaciotaki-Boussalis
Maj Mirmirani
Khosrow Rad
Mauricio Morales
Efrain Velazquez

California State University, Los Angeles
5151 State University Dr.
Los Angeles, CA 90032

Anastasios Chassiakos
Jose-A lberto Luzardo

California State University, Long Beach
1250 Bellflower Blvd.
Long Beach, CA 90840-5602

ABSTRACT

The 3-dimensional model for a segmented reflector telescope is developed using finite element techniques. The structure is decomposed into six subsystems. System control design using neural networks is performed. Performance evaluation is demonstrated via simulation using PRO-MATLAB and SIMULINK.

1. INTRODUCTION

Future astronomical space missions will require high-performance optical systems. Such optical systems will necessarily have large apertures for high-precision performance making the size of the reflectors very large. Due to practical considerations such as time, cost and complexity of fabricating large-aperture telescopes, as well as launch vehicle size. weight and power constraints, future telescopes will be made of precision-segmented reflectors. A segmented mirror reflector consists of mirror panels which, when formed together, become a parabolic primary m irror that magnify the images from space. These mirror panels are easily manufactured, and deployable in space when the proper orbit is achieved.

With the advantages of the segmented reflector telescopes, shortcomings are also present. The large size of these telescopes make the structure flexible to external forces such as thermal fluctuations and solar disturbances. It becomes apparent that development of control concepts and extensive performance evaluation via simulation in an environment characterized by various dynamic disturbances is a necessity. The control design challenge is to make the segmented reflector perform as a monolithic reflector. This is done via high-precision figure control which would maintain the surface of the reflector to within a specified tolerance of the calibrated reference position.

Due to the large size of the telescope structure, it becomes apparent that control system design based on conventional methods is exceedingly difficult. The mathematical model of the structure involves hundreds of states and use of centralized control ler could not accomplish figure control according to specifications. Decentralized control has been used by several researchers in the recent years to overcome the difficulties due to the dimensionality problems that arise when dealing with large-scale systems [5]. This approach has been taken here to accomplish control of the segmented reflector. Specifically, the structure has been decomposed into six smaller-order subsystems. The decentralization is performed physically by slicing the structure vertically and isolating every mirror panel along with its associated structural member.

The control design has been performed using PID [1], pole-placement, H_2 (LOG), H-infinity and neural networks control. The neural network based control is discussed in the present paper. The control law is developed at the local level and performance evaluations are performed utilizing the control law of the isolated subsystems and the interaction among them.

Section 2 contains the mechanical and structural design of the structure, section 3 lists the control system requirements, section 4 contains the mathematical model, section 5 describes the decentralization of the structure, section 6 contains the neural network based control design, section 7 contains the computer architecture of the structure, and section 8 contains the summary of the results.

2. MECHANICAL AND STRUCTURAL DESIGN

The Control and Structures Research Laboratory (CSRL) segmented reflector testbed is an experimental apparatus capable of addressing the technical challenges presented by a complex three-dimensional structure such as a large segmented optical system. To validate both control strategy and implementation for realistic systems, a set of requirements have been used to design the testbed [2]. These requirements are based on various missions within NASA's Precision Segmented Reflector Program (PSR) [1], They are also based on the requirements used for similar projects, including JPL's PSR and Lockheed's ASCIE testbeds. Since the CSRL testbed is a control-system oriented instrument, requirements are selected mainly to demonstrate a high level of disturbance attenuation rather than optical performance.

PERFORMANCE: Performance of the testbed is required to be of comparable quality to that of an actual system. The testbed is designed to perform the essential functions needed for the various system missions including static and dynamic segment alignment, fine pointing and vibration suppression.

DYNAMICS: The structure is designed to approximate the fundamental dynamic characteristics of a three-dimensional large structure, i.e. low-frequency modes, high modal density, and global mode shapes that properly reflect the coupling of the sub-elements of the structure. The system is designed to accommodate interdisciplinary experiments in validation of control algorithms, CSI, optics, electronics, actuators, sensors, and distributed multiprocessor design and implementation. The system is designed to demonstrate physical and mathematical decentralization and accommodate development of control algorithms related to decentralized control technique.

2.1 CSRL system description. Figure 1 is a schematic illustration of major features of the testbed, including the primary and secondary mirrors, the actuators, the edge sensors. The active optical elements are the primary-mirror segments which interact dynamically with the actuators, sensors and the supporting structure in an integrated way. The primary mirror is a 2.63 m diameter dish supported on a lightweight, flexible truss structure. The optical system emulates that of an f / 2.4 m Cassegrian telescope. The major components of the CSRL testbed are discussed bellow.

STRUCTURE: One of the most fundamental design goals has been a strong, light-weight truss structure whose structural-dynamic characteristics are representative of a large, flexible space-borne system. These include low frequency modes, high modal density and global mode shapes that properly reflect the coupling of the sub-elements of the structure [2]. Therefore, the requirements for the design of the truss, in addition to the dimensional constrains, included a careful trade-off between the need for the structure to support itself in the 1-g laboratory environment versus the need to keep the frequency of the first mode as low as possible. Multi-criteria optimization technique based on Pareto optimality concept was employed to accomplish this objective. The overall dimensions are 2.275 m across and 0.580 m thick. The structure is made of nine groups of stainless steel truss elements ranging in size from 0.921 m to 0.414 m. There are 60 elements and 21 nodes. The truss is supported on a specially designed isolation platform.

SEGMENTED PRIMARY MIRROR : The CSRL primary mirror is designed to emulate the critical properties of a real segmented mirror. These properties include segmentation geometry, inter-segment spacing, segment mass, inertia and stiffness, and optical focal ratio. The seven segment primary mirror consists of a ring of six actively controlled hexagonal segments surrounding a fixed center segment that acts as a reference. Because the testbed is control-system oriented, and because of difficulty and added expense of fabrication of actual optical-quality segments made from glass, the segments will be fabricated from flat honeycomb aluminum plates. The active segments are attached to segment-positioning actuators with special three-degree-of-freedom flexures. These flexures permit individual segments to have two rotational degree of freedom (tilt) and one transitional degree of freedom (piston). Each segment is controlled by three actuators and the entire primary has a total of 18 actuators. The relative displacement between the edges of adjacent segment unmeasured by an ensemble of 24 edge sensors. The edge sensors provide information about a segment's relative displacement as well as absolute displacements from the fixed center reference segment.

SEGMENT-POSITIONING ACTUATORS: Use of high performance segment-positioning actuators are the key to precision control of the CSRL testbed primary mirror. These actuators must have extremely low noise level, be able to generate substantial force over a wide mechanical range and support the weight of a segment in a 1-g field. They must also have a bandwidth sufficient to accommodate the spectrum of expected disturbance and to support robust control of the system. In addition, they should be able to actuate free of friction, and minimize thermal energy dissipation. These actuators must be fitted with collocated positioning sensors and/or accelerometers, be modular and compact in size and easily interface with the structure. Because conventional actuators are unable to meet one or more of the above performance requirements a voicecoil design has been especially developed for the CSRL testbed. These actuators are being fabricated by Northern Magnetic, Inc. in Southern California. Some of the mechanical features include especially designed disk flexures instead of conventional bearings and an off load spring is to minimize actuator force requirements and thermal energy dissipation when the actuators are holding the weight of the segment. The actuators have a bandwidth of 0-150 Hz., positioning resolution of 0.1 micrometer and a maximum force output of 54 Newtons.

ACTIVE SECONDARY MIRROR: The CSRL testbed secondary reflector design consists of a 12.5 in mirror supported by a tripod that is attached to the primary truss at three points. The mirror is designed to provide two-axis, active beam-steering control. An active closed-loop control system is being designed that is capable of aligning the secondary to the focal plane, removing all relative angular motion between the secondary and the reference center segment of the primary structure. The secondary mirror is supported by isolation springs attached to the secondary structure. Three reluctance actuators located 120 degrees from each other provide for three degrees of freedom (tip, tilt, piston) motion. Three position sensors are used in combination with the actuators to control the position of the mirror.

2.2 **Structural optimization.** Pareto optimality concept [4] was used to design a structure which represents the "best" trade off between flexibility and strength. The panel surface distortion due to gravity as measured by the RMS distortion of the upper truss nodes and total mass of the structure were selected as two criteria for optimization. A set of Matlab subroutines which use finite element data to arrive at an optimal solution were developed. Two sets of geometric parameters were allowed to vary at specified increments to obtain variations of the baseline structure. RMS values and total mass were calculated for each resulting structure. The structures with different geometric characteristics plotted as a collection of points in the objective space show a Pareto optimal pattern on the boundary of the region (Figure 2). Only points on the left of the dotted area from point A to point C represent Pareto optimal solutions. Point A represents the structure with minimum RMS surface distortion, while point C represents the minimum weight structure. The optimal structure, represented by point B, has a total mass of 146.9 Kg and an RMS surface distortion of 44.6 microns representing a simultaneous improvement of 52% and 75.4% respectively over the baseline design

2.3 **Modeling and structural dynamics.** IMOS (Integrated Modeling of Optical Systems) program [4] and MSC/NASTRAN software were used to develop finite element models for the CSRL testbed. The models include the primary and the secondary truss structures, the panels, the joints, the fittings, and the actuators. The eigenvalue analysis of the system showed that the lowest natural frequency of the structure is at 10.3 Hz. Figure 3 illustrates the frequency histogram for the first 100 modes of the structure indicating that the dynamic characteristics of the CSRL structure are similar to those of a large flexible structure characterized by low fundamental frequency and high modal density. Figure 4 shows mode shapes representing the first significant primary structure frequencies.

3. **CONTROL SYSTEM REQUIREMENTS**

The following requirements were developed at CSRL for the control system:

- Line-of-sight (Pointing) accuracy of 2 arc seconds.
- Figure maintenance to within l micron (rms distortion) with respect to calibrated surface,
- Control Bandwidth 15-30 Hz.
- Use voice coil actuators to provide an actuator bandwidth of 100-200 Hz.
- Control up to first 20 modes reduce spil lover effect due to neglected modes and dynamics,
- Attenuate vibrations due to gravity, thermal, seismic effects, etc.
- Minimize the "Disturbance" effect of the active control.

4. **MATHEMATICAL MODEL**

The equation of motion for the system under consideration is given by:

$$M\ddot{q} + Kq = B_1 u + B_2 f$$

where M is a positive definite symmetric mass matrix, K is a positive semi-definite symmetric stiffness matrix, B_1 is a control influence matrix, B2 is a disturbance influence matrix, and q is the vector of physical coordinates, i.e.. panel displacements. The generalized mass and stiffness matrices are developed via finite element modeling (FEM).

The segmented reflector telescope structure consists of 42 nodes and each node introduces 6 degrees of freedom. Control and performance evaluation of such structure is an exceedingly difficult task. To reduce the number of degrees of freedom and still maintain accuracy, a method called Guyan reduction is used here to reduce the system mass and stiffness matrices by omitting the x and y degrees of freedom of the 42 truss and panel nodes. The reduced mass and stiffness matrices are further used for decentralization and control design.

5. **DECENTRALIZATION**

Large space structure control design is characterized by high dimensionality and complexity making the controller one of a large order with attendant complexity. Considering that the original state-space model is derived via finite element programming which already uses many assumptions about structural elements, their masses, mass distribution, other properties, and interconnections, etc., the original state space model itself can be assumed to be but an approximation of the real structure. Therefore, instead of corrupting the models further by eliminating more of the available states, the approach of decentralized control appears to be a more realistic way of alleviating the dimensionality problem. The controllers for individual panels are derived using all of the available measurements from the entire structure. Decentralized control is a better approach in terms of designing a realistic controller because it is not based on neglecting available information. Also, in terms of reducing the control spillover effect, decentralized control is better compared to model reduction achieved by drastically reducing the number of states. It is well known that control spillover resulting from neglected modes and dynamics can potentially destabilize a system.

One of the most important aspects of decentralized control is in fault tolerance. In the decentralized approach controllers are designed for individual subsystems while incorporating the interactions among them. In the event of a controller failure, the system can gracefully degrade into one where via proper decentralization, the adjacent panel controllers may compensate for the failed controller. The decentralization could be based on several factors such as time-scale based decentralization, frequency-scale based decentralization or structure-based decentralization. [n this paper the natural symmetry of the structure is exploited to decompose the system into smaller subsystems, each of a much lower order. It has merits in reducing the controller size and complexity thereby easing computational burden on the processor. Simpler control algorithms will in turn lead to simpler hardware implementation. The reduced version of the structure is decomposed into six subsystems as follows:

$$x_i = A_{ii} x_i + E_i x$$

where E_i is the subsystem interactions including the effects of disturbances.

The isolated panel components arc given by $\dot{x}_i = A_{ii} x_i$, where $A_{ii} = \begin{bmatrix} 0 & I \\ -\omega_i^2 & -2\zeta_i \omega_i \end{bmatrix}$.

6. NEURAL NETWORK BASED CONTROL

Two neural network architectures were developed and tested in simulation for the problem of disturbance rejection of the large segmented space reflector, The development and simulation results of these architectures are presented in the current section. The *first controller* is a novel neural network controller (NNC) whose parameters are adjusted on line [7]. The control algorithm is simple and can be implemented in real time. Unlike other NNCs that are reported in the literature, the proposed neural network controller requires relatively few neurons and its learning algorithm is f'aster than backpropagation. Stability analysis by a Lyapunov approach is used to determine the convergence properties of the algorithm. The stability is guaranteed with rather mild conditions and certain prior knowledge of the plant to be controlled. The proposed adaptive control consists of a neural network placed in the feedback loop and an adaptation law to adjust the parameters of the net. The *second controller* is a feedforward two-layer neural network. The net work is trained off-line to emulate a dynamic compensator. The training is done by classical back-propagation.

6.1 **Adjustable neural network controller.** The proposed control system is shown in Fig. 5 and is based on part of the doctoral dissertation of J.-A. Luzardo [7] currently in progress. In the following, we describe its main characteristics.

The plant to be controlled is assumed to be *almost strictly positive real (ASPR), i.e.* there exists an output feedback gain matrix K such that the closed loop system $A - BKC$ is *strictly positive real* [6]. It is noted that the value of K *is* not needed for implementation, only its existence is required.

The neural network controller of Fig. 5 is a two-layer network with onc hidden layer ($u = N(e)$). The internal network topology is arranged to provide the following outputs (control inputs to the plant):

$$u_i = \sum_{j=1}^{p} \left(\sum_{k=1}^{l} c_{ijk}(t)\sigma(\omega_{ijk} e_j + \theta_{ijk}) \right)$$

where u_i is the *i-th* component of u and e_j is the *j-th* component of $e = y_m - y$, and $\sigma(z) = 1 / (1 + e^{-z})$ It is noted that the parameters c_{ijk} are time varying, while the parameters ω_{ijk} and θ_{ijk} are constant. For notational simplicity we denote $\sigma(\omega_{ijk} e_j + \theta_{ijk})$ by σ_{ijk}. Then $u_i = \Sigma_i^T \alpha_i$, where $\Sigma_i = [\sigma_{i11} \cdots \sigma_{i1l} \cdots \sigma_{ipl}]^T$ and $\alpha_i = [c_{i11} \ldots c_{i1l} \cdots c_{ipl}]^T$. Using these definitions, the vector u can be written as

$$u = \begin{bmatrix} \Sigma_1^T & & \\ & \Sigma_2^T & \\ & & \ddots \\ & & & \Sigma_p^T \end{bmatrix} \begin{bmatrix} \alpha_1 \\ \alpha_2 \\ \vdots \\ \alpha_p \end{bmatrix} = \Phi\alpha$$

The adjustable parameters of the neural network controller are adjusted according to the following adaptation law: $\dot{\alpha} = \Gamma_1 \Phi^T e - \Gamma_1 \Gamma_2 \alpha$, where Γ_1 and Γ_2 are two symmetric positive definite matrices chosen according to design criteria. Under these conditions it is proven by Luapunov function arguments that the neural network controller will keep the closed loop system stable and the signals in the closed loop will remain bounded.

6.2 **Simulation results.** The *ASPR* condition in the case of a flexible space structure is guaranteed if the sensors and actuators are collocated and if the measured output is a combination of rate and position measurements [6]. Simulations were performed on the telescope model, under these assumptions, and some of' the simulation results are shown in Fig. 6. The results shown are for a three-panel subsystem, when three sinusoidal disturbances were applied 10 each panel. Only the responses for panel 2 are displayed. The dashed line is the open loop response, whereas the solid line is the response under the neural network controller. It is seen that the neural controller attenuates the response due to disturbance by a factor of 10 or higher. Similar rc.suits were obtained for the remaining panels and for other disturbances with different characteristics.

6.3 **Neural network controller trained by back propagation.** This is a neural controller concept that was investigated as an alternative to the adjustable neural network controller of the previous subsection. As a first step towards the development of this controller,it was decided that the control ler block be trained off-line by standard back propagation, and that its performance be evaluated before proceeding to designing on-line training algorithms. Thus, it was assumed that the system is known, hence there is no need an for on-line neural identifier, and a dynamic compensator was designed to control the known system. The neural controller block was trained off-line to emulate the dynamic compensator, based on input/output data from the compensator. The resulting neural network was placed in the forward loop as a neural implementation of the dynamic compensator, and several simulation studies were performed to evaluate its performance. The simulation tests presented here are for a two-panel subsystem. A sinusoidal disturbance with frequency close to the natural frequency of the simplified model is chosen. Fig. 7 shows the regulation ability of the neural controller, for panel 1. The dashed linc represents the positions with the controller off (open loop), whereas the solid line represents the positions with the controller on (closed loop). It is again seen that the controller reduces the disturbance effects by almost a factor of 10.

7. COMPUTER ARCHITECTURE

The drive electronics used in the CSRL testbed is for the purpose of processing the analog output of sensors and interfacing with the segment positioning actuators. The drive electronics is in charge of real-time processing and data acquisition. The computer and graphic setup includes a DSP, a PC and two SUN stations. Figure 8 illustrates the overall computer architecture block diagram. The DSP is the main computational unit and it is responsible for real time control processing, signal generation, and real time directory memory. Access data transfers to a 256 K bytes internal memory block resides on the DSP. The DSP and the SUNS are used to monitor the CSRL experiments via the graphical display of the Kaman sensors reading, the actuator commands, and the mirror segments piston and tilt misalignment. The input/output unit is composed of two 32-channels 16 bit analog to digital and two 18-channel 16-bit digital to analog converters.

8. SUMMARY

A lightweight rigid structure has been designed using Pareto optimality technique. The structure exhibits dynamic behavior of a large flexible structure characterized by low fundamental frequency and high modal density. The structure has been decomposed into six subsystems. The control law is designed using the individual subsystems as well as the interconnection properties among them. The control design is performed using neural net works. Performance evaluations are performed utilizing PRO-MATLAB and SIMULINK. The *first neural network controller* adjusts its weights on-line and requires measurements of the positions and velocities, and that the actuators and sensors be collocated. Under these conditions the ASPR condition is satisfied, allowing the NNC to be implemented. The NNC is simple because it adjusts the coefficients of the linear layer (output layer) of the NN. The internal parameters of the sigmoids (hidden layer) are fixed in accordance with the operation range of the system. A special consideration is taken to uniformly distribute the centers of the sigmoids all over the range of operation. The simulation results present satisfactory transient responses and a fast adaptation, although the neural weights were all initialized to zero. As predicted by theory, all the signals remain bounded and all position errors remain small, in the presence of external disturbances. The results from *second neural controller* suggest that a strategy utilizing prior information about the structure, such as a good model, can be very effective. A dynamic compensator designed from the numerical model is used to train a feedforward neural network. The trained network is shown through simulations to have good disturbance rejection properties and good step following. The weights of the trained network can be used as an initialization point for subsequent on-line weight adaptation algorithms.

9. ACKNOWLEDGMENTS

The research described in this paper was carried out at the Control and Structures Research Laboratory and was supported by the National Aeronautics and Space Administration under grant # NAGW-4103.

10. REFERENCES

[1] Ryaciotaki-Boussalis, Z. Wei, and M. Mirmirani, "Decentralization and PID Controller Design for Large Space Borne Telescopes," IASTED Conference on Modeling and Simulation, Pittsburgh 1995.
[2] Aubrun, Jean-Noel, et al. "Active Control for Segmented Mirror Optical Systems," Research and Development Division, Lockheed Missiles and Space Company, Palo Alto, California.
[3] Hahn, M., Mirmirani, M., Boussalis, H., "Optimal Design of a Truss Structure for a Segmented Reflector," ASME Conference, Boston, 1995.
[4] Stadler, W., Editor, "Multicriteria Optimization in Engineering and in Science," Plenum, NY, 1988.
[5] H. R. Boussalis, C. H.Ih, "Modeling and Stability of Segmented Reflector Telescopes: A Decentralized Approach," Proc 23rd Asilomar Conference, 1989.
[6] Kaufman, H., Bar-Kana, I., and Sobel, K. "Direct Adaptive Control Algorithms." Springer, 1994.
[7] Luzardo, J-A. "Neural Networks for Approximation and Control of Continuous Nonlinear Dynamical Systems.", Ph.D. thesis, Dept. of Mathematics, The Claremont Graduate School, Claremont, CA. 1996,

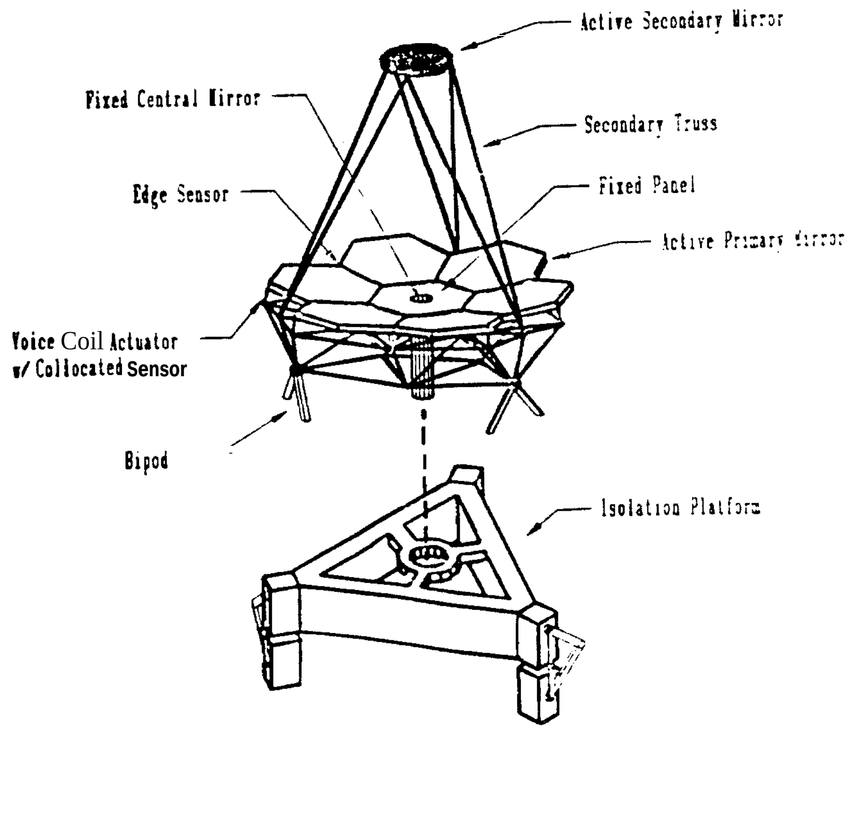

Figure I: The CSRL segmented reflector

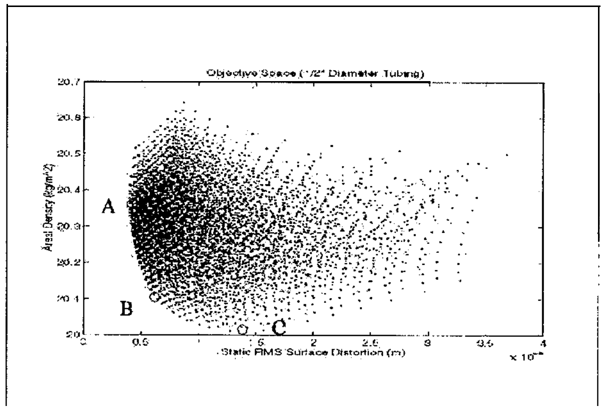

Figure 2: Truss optimization results

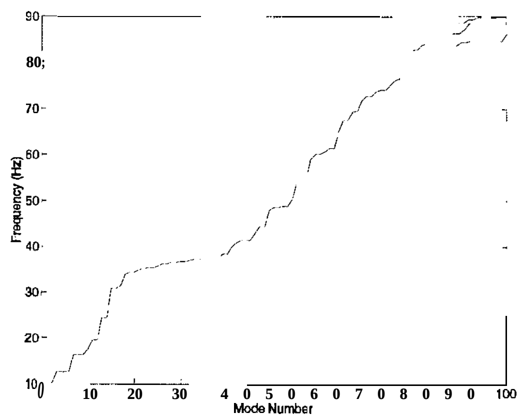

Figure 3: Frequency histogram of the CSRL structure

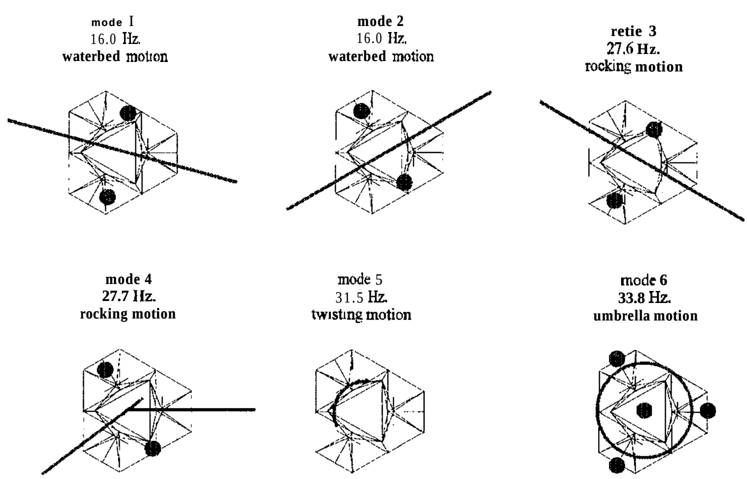

Figure 4: First six mode shapes of the CSRL structure

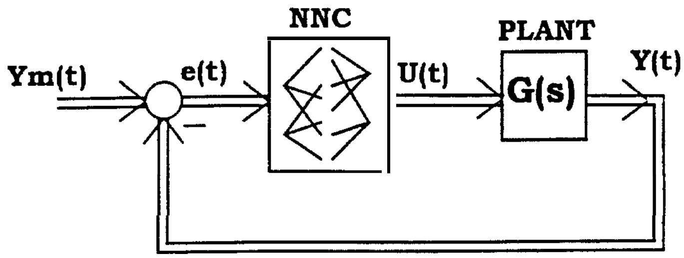

Fig. 5: Block diagram of the neural network controller

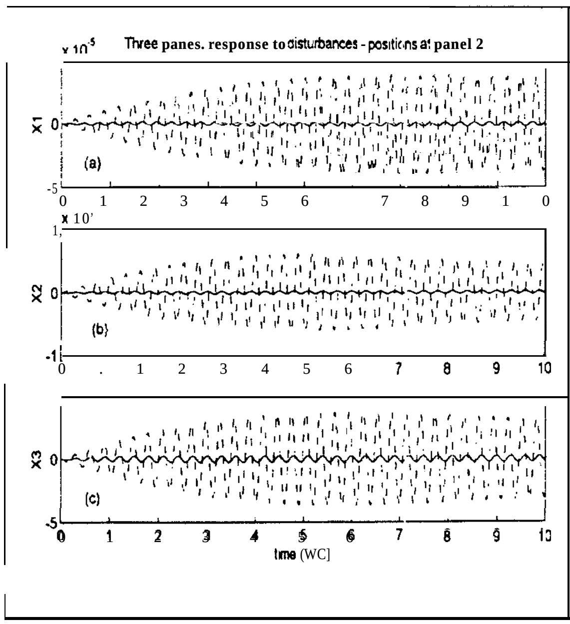

Fig. 6: Adjustable neural network controller. Open loop (dashed line) and closed loop (solid line) responses under sinusoidal disturbances

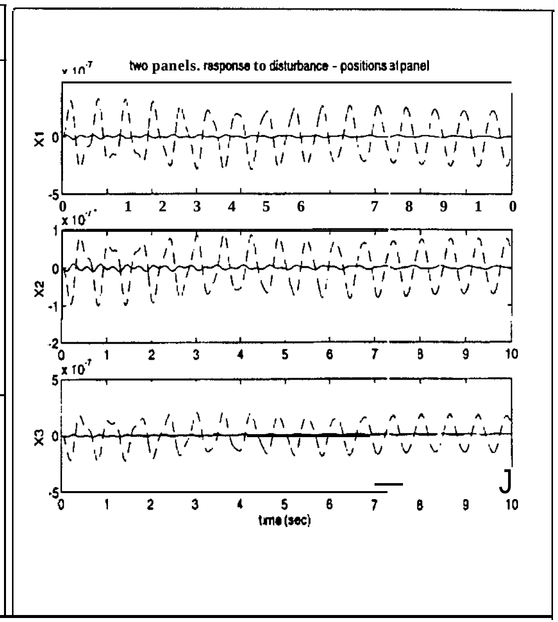

Fig. 7: Controller trained by back propagation. Open loop (dashed line) and closed loop (solid line) responses under sinusoidal disturbances

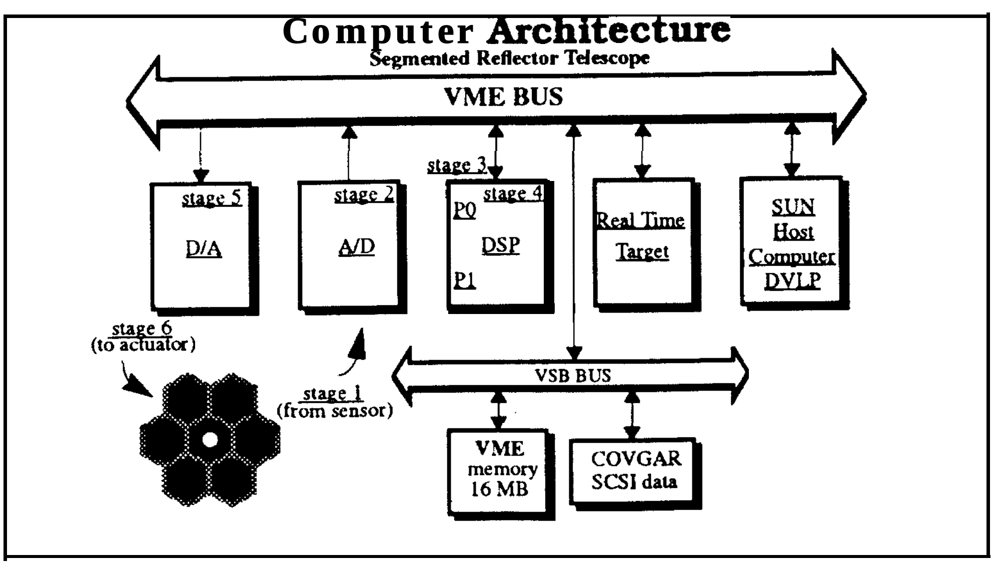

Figure 8